Prostate Cancer Cell Phenotypes Remain Stable Following PDE5 Inhibition in the Clinically Relevant Range

William Hankey [a,b], Benjamin Sunkel [c], Fuwen Yuan [a,b], Haiyan He [a,b], Jennifer M. Thomas-Ahner [c], Zhong Chen [a,b], Steven K. Clinton [c], Jiaoti Huang [a,b], Qianben Wang [a,b,*]

[a] Department of Pathology, Duke University School of Medicine, Durham, NC 27710, USA
[b] Duke Cancer Institute, Duke University School of Medicine, Durham, NC 27710, USA
[c] Department of Internal Medicine, The Ohio State University College of Medicine, Columbus, OH 43210, USA

ARTICLE INFO

ABSTRACT

Widespread cGMP-specific phosphodiesterase 5 (PDE5) inhibitor use in male reproductive health and particularly in prostate cancer patients following surgery has generated interest in how these drugs affect the ability of residual tumor cells to proliferate, migrate, and form recurrent colonies. Prostate cancer cell lines were treated with PDE5 inhibitors at clinically relevant concentrations. Proliferation, colony formation, and migration phenotypes remained stable even when cells were co-treated with a stimulator of cGMP synthesis that facilitated cGMP accumulation upon PDE5 inhibition. Surprisingly, supraclinical concentrations of PDE5 inhibitor counteracted proliferation, colony formation, and migration of prostate cancer cell models. These findings provide tumor cell-autonomous evidence in support of the field's predominant view that PDE5 inhibitors are safe adjuvant agents to promote functional recovery of normal tissue after prostatectomy, but do not rule out potential cancer-promoting effects of PDE5 inhibitors in the more complex environment of the prostate.

Introduction

cGMP-specific phosphodiesterase 5 (PDE5) inhibitors such as sildenafil block the enzymatic degradation of cyclic guanosine monophosphate (cGMP), a nucleotide that functions as a second messenger in multiple cellular signaling pathways. Reports have linked PDE5 to cancer development and progression in multiple ways that first emerged from studies in melanoma cells [1]. PDE5 promotes melanoma cell growth [2,3] but prevents invasion [2]. In contrast, PDE5 effects in other cell types are primarily antiapoptotic [4] so that PDE5 inhibitors can act as sensitizing agents to promote therapeutic killing of cell models of chronic lymphocytic leukemia [5], acute myeloid leukemia [6], multiple myeloma [7], and head and neck squamous cell carcinoma [8]. These findings are also consistent with studies of cGMP, which can either stimulate or inhibit cellular proliferation and apoptosis, depending on the cancer type [9–11]. Thus, the ability of the PDE5/cGMP pathway to promote or counteract tumorigenesis may depend on cellular context.

PDE5 inhibitors have become increasingly widespread for the treatment of erectile dysfunction and for the recovery of reproductive health among prostate cancer patients who have undergone surgery. Emerging opportunities to associate PDE5 inhibitor use with incidence and prognosis of malignant disease have uncovered associations between PDE5 inhibitor use and decreased incidence of prostate cancer, benign prostate hyperplasia, and elevated PSA [12]. On the other hand, a 2015 publication by Michl et al. detected an association between PDE5 inhibitor use and increased prostate cancer recurrence after radical prostatectomy [13], raising a clinical concern over the safety of their use as adjuvant agents among these patients. Two replication studies in similar patient populations could not reproduce the statistical significance of this finding nor detect a dose-dependent effect [14,15]. Yet lingering uncertainty around the safety of PDE5 inhibitor application in the context of prostate cancer motivated the present study to interrogate tumor cell autonomous effects by screening prostate cancer cell lines for PDE5A expression and exposing them to clinically relevant concentrations of PDE5 inhibitors.

The present study has been designed to provide a mechanistic point of view on the recent epidemiology studies associating PDE5 inhibitor use with prostate cancer recurrence. These experiments test the hypothesis that PDE5 inhibitor administration in the clinical range can trigger cGMP accumulation and cell autonomous phenotypic changes in prostate cancer cells. These new data are relevant to the prostate cancer field and to the study of PDE5 inhibitors for broader clinical applications in that they help establish how these agents influence tumor cell autonomous phenotypes. In attempting to find mechanistic evidence at the tumor cell level consistent with a role in promoting prostate cancer recurrence, these studies shed light on the safety of the continued use of PDE5 inhibitors by prostate cancer patients following radical prostatectomy.

* Address all correspondence to: Qianben Wang, Room 1027A, GSRB1, Box 103864, 905 S. LaSalle St., Durham, NC 27710.
E-mail address: qianben.wang@duke.edu. (Q. Wang).

Materials and Methods

Cell Lines

22Rv1 cells were maintained in RPMI 1640 medium + 10% fetal bovine serum, and all experiments were completed with cells between passages 10 and 30. PC-3 cells were also maintained in RPMI 1640 medium + 10% fetal bovine serum, and all experiments were completed with cells between passages 20 and 40. LNCaP cells were similarly maintained in RPMI 1640 medium + 10% fetal bovine serum, and all experiments were completed with cells between passages 20 and 40. LNCaP-abl cells were maintained in phenol red-free RPMI 1640 medium + 10% charcoal-stripped fetal bovine serum, and all experiments were completed with cells between passages 60 and 72. All cell lines had previously been confirmed to be free of mycoplasma contamination, were maintained in antibiotic-free medium, and were immediately discarded and replaced if any sign of contamination was observed.

Primary aortic smooth muscle cells were obtained through ATCC (catalog # PCS-100-012) and cultured in Vascular Cell Basal Medium (ATCC PCS-100-030) supplemented with 5 ng/ml recombinant human FGF-basic, 5 μg/ml recombinant human insulin, 50 μg/ml ascorbic acid, 10 mM L-glutamine, 5 ng/ml recombinant human EGF, 5% fetal bovine serum, and 50 U/ml penicillin–streptomycin (ThermoFisher Scientific catalog # 15070063). All experiments were completed with cells between passages 6 and 12.

Western Blotting

Cells were plated in six-well plates at 1×10^6 (22Rv1), 7×10^5 (LNCaP, LNCaP-abl), 5×10^5 (PC-3), or 2.5×10^5 (primary aortic smooth muscle) cells/well. After approximately 24 hours, when cells had reached ~60% confluence, medium was replaced with warm, drug-containing medium, followed by incubation for either 20 minutes (primary aortic smooth muscle cells) or 60 minutes (prostate cancer cell lines) in a 37°C incubator.

Cells were collected by scraping into PBS, centrifuged at $300 \times g$ to pellet, and then lysed with 50 μl cold RIPA buffer (50 mM Tris–HCl pH 8.0, 150 mM NaCl, 0.1% SDS, 1% NP-40, 0.5% sodium deoxycholate) supplemented with protease inhibitor (Millipore catalog # 4693116001) and phosphatase inhibitor (Millipore catalog # 4906837001) cocktails. After 20-minute incubation on ice and maximum speed centrifugation, supernatant was isolated and subjected to Bradford assay (BIO-RAD catalog # 5000006) to determine protein concentration. Samples were diluted to a consistent concentration for each experiment, with 20 μg to 50 μg total protein loaded per lane of a 4%-15% polyacrylamide gradient gel (BIO-RAD catalog # 456-8084) run in Tris/glycine/SDS buffer. Transfer to PVDF was performed overnight at 30 V and 4°C. Blocking in 5% milk in TBST took place over 2 hours, followed by overnight incubation with primary antibody in 5% milk in TBST. Blots were washed five times for a total of approximately 30 minutes and then subjected to secondary antibody incubation (1:5000 or 1:10,000) in 5% milk in TBST for 2 hours at room temperature. Blots were then washed five additional times for a total of approximately 30 minutes and developed using SuperSignal West Pico PLUS Chemiluminescent Substrate (ThermoFisher Scientific catalog # 34580). Images were generated using either Amersham ECL film (GE Life Sciences catalog # 28906838) or Li-Cor C-DiGit Western blot scanner.

Primary antibodies were obtained from Santa Cruz Biotechnology (PDE5A H-120 catalog # sc-32884, PRKG1/cGKIα/β G-3 catalog # sc-271766, p-CREB-1 Ser133 catalog # sc-7978-R, CREB-1 C-21 catalog # sc-186, and GAPDH 6C5 catalog # sc-32233), Cell Signaling Technology (Phospho-VASP Ser239 catalog # 3114S and VASP 9A2 rabbit mAb catalog # 3132S), and Enzo Life Sciences (Calnexin polyclonal antibody catalog # ADI-SPA-860-F). Calnexin was used as a stable loading control for multiple treatments within individual cell lines, while GAPDH was used as a relatively stable loading control across multiple cell lines. Secondary antibodies were obtained from Li-Cor (WesternSure Goat Anti-Rabbit HRP, catalog # 926-80011, and WesternSure Goat Anti-Mouse HRP, catalog # 926-80010).

Drug Treatments

Sildenafil citrate (Millipore Sigma catalog # PZ0003-25MG), vardenafil hydrochloride trihydrate (Millipore Sigma catalog # SML2103-50MG), and riociguat (Millipore Sigma catalog # G-6188-100MG) were each dissolved in DMSO at stock concentrations of 100 mM and subsequently diluted further in DMSO as necessary to generate $1000 \times$ stock solutions for each condition of interest. Thus, they were always added to prewarmed medium at a final DMSO concentration of 0.1%, regardless of the final drug concentration. Drugs were added only to prewarmed medium to ensure their complete solubility. 8-Bromo-guanosine 3′,5′-cyclic monophosphate sodium salt (Millipore Sigma catalog # B1381-25MG) and 8-bromoadenosine 3′5′-cyclic monophosphate sodium salt (Millipore Sigma catalog # B7880-25MG) were diluted in ultrapure distilled water to stock concentrations of 100 mM, while C-type natriuretic peptide (Millipore Sigma, catalog # N8768-.5MG) was diluted in ultrapure distilled water to a stock concentration of 1 mM.

WST-1 Assays

Cells were trypsinized, counted, and seeded into black polystyrene 96-well plates (Millipore Sigma catalog # CLS3603-48EA) at densities of 2500 (for 22Rv1), 3000 (for LNCaP and LNCaP-abl), or 1500 (for PC-3) cells per well in a volume of 100 μl per well. Only the 60 wells at the center of the plate were used, while the remaining 36 wells along the border of the plate were filled with 100 μl of media instead, to protect the inside cells from evaporation. Three separate 96-well plates were seeded in this fashion for each cell line/experiment to facilitate the use of separate plates for the day 0, day 2, and day 4 measurements. Twenty-four hours after cell seeding, the original medium was removed and replaced with prewarmed drug-containing medium. Six technical replicates of each treatment were performed. Measurements were made at the time the drug-containing medium was added (day 0), as well as 2 days and 4 days after the addition of drug. For each measurement, 10 μl WST-1 reagent was added to each 100-μl well, and the plate was incubated for 2 hours in the 37°C incubator. Measurement of absorbance at 440_{nm} was then made on a SpectraMax M3 microplate reader. In general, only the 32 wells at the very center of the plate were included in the statistical analysis to limit the evaporation-based variability associated with wells at edges of the plate. Four measurements were analyzed for each of eight drug treatments. Each biological replicate generated four technical replicates that were analyzed by a two-tailed unpooled (Welch's) version of The Student's t test to evaluate statistical significance.

Colony Formation Assays

Cells were trypsinized, counted, and seeded into six-well plates with 200 cells and 3 ml of medium per well. Twenty-four hours after seeding, medium was replaced with warm drug-containing medium. Cells were incubated 11 (PC-3), 14 (22Rv1), 18 (LNCaP-abl), or 21 (LNCaP) days after addition of drug-containing medium. Colonies were washed with PBS and subjected to methanol-based fixation and subsequent staining with eosin Y and methylene blue/azure A using the Richard-Allan Scientific Three-Step Stain Set (Thermo Fisher Scientific catalog # 3300). Visualized colonies were rinsed gently with water and allowed to dry prior to camera-based imaging and counting using ImageJ2 [46]. Each biological replicate consisted of three technical replicates that were analyzed using a two-tailed unpooled (Welch's) version of The Student's t test to evaluate statistical significance.

Wound Healing Assays

Cells were trypsinized, counted, and seeded into a four-well 35-mm μ-dish (Ibidi catalog # 80466) at densities of 1.1×10^5 (for 22Rv1 and LNCaP), 1.0×10^5 (for LNCaP-abl), or 7.7×10^4 (PC-3) cells per well. Cells were incubated either 24 hours (for 22Rv1 and PC-3) or 48 hours

(for LNCaP and LNCaP-abl) after seeding to generate a well-adhered and confluent monolayer. Sterile tweezers were used to carefully remove the insert and generate a "wound" with four sections. The monolayer was washed once (for 22Rv1 and PC-3 cells only, not for LNCaP or LNCaP-abl) with media containing 2% fetal bovine serum to remove cell debris. Then, 2 ml of warm drug-containing media (also 2% fetal bovine serum) was added. The four sections of the wound were each photographed at $10\times$ magnification using an EVOS microscope camera (Life Technologies). Plates were then incubated at 37°C for 1 day (for fast-migrating PC-3) or 4 days (for slow-migrating 22Rv1, LNCaP, and LNCaP-abl) before a second set of pictures was taken. Images were used to calculate the percent of each wound remaining unhealed relative to the original distance between the two sides in the first set of pictures. Each biological replicate generated four technical replicates that were analyzed by a two-tailed unpooled (Welch's) version of The Student's *t* test to evaluate statistical significance.

siRNA-Based Gene Silencing

Cells were seeded in six-well plates approximately 24 hours prior to transfection at a density of 3.33×10^5 cells/well. Transfections were performed using 7.5 μl per well of Lipofectamine RNAiMAX reagent (ThermoFisher Scientific catalog # 13778075) and 50 pmol per well of pooled siRNA, exactly following the manufacturer's recommended protocol. Catalog numbers from Horizon Discovery were L-007667-00-0005 (*PDE5A*), L-003400-00-0005 [androgen receptor (*AR*)], L-004693-00-0005 [ubiquitin conjugating enzyme E2 C (*UBE2C*)], or D-001810-10-05 (nontargeting control). Cells were harvested 48 hours after transfection for Western blot analysis or for seeding for WST-1 and wound healing assays.

ELISA Assays

cGMP and cAMP assays were performed using the Cyclic GMP ELISA Kit (catalog # 581021) and Cyclic AMP ELISA Kit (catalog # 581001) from Cayman Chemical according to the manufacturer's protocols. Briefly, 22Rv1 and PC-3 cells were stimulated in six-well plates with drug-containing medium for 60 minutes in the 37°C incubator. Medium was removed, and 0.5 ml of an acidic (0.1 M HCl) solution was added to each well to harvest and protect intracellular cGMP or cAMP. HCl was incubated with the cells for 20 minutes at room temperature with gentle rocking, then scraped to collect and pipetted up and down 15 times to achieve homogeneity. The suspension was centrifuged for 10 minutes at room temperature at $1000\times g$, and 750 μl of supernatant was isolated. Samples were diluted 1:6 in the kit-provided $1\times$ ELISA buffer. Dilutions were also prepared for 0.1 ml HCl as a negative control and for the kit-provided cGMP or cAMP standards in the linear ranges of the assays. An optional acetylation reaction was performed to increase the sensitivity of the assays. The reaction was performed for each dilution and each cGMP or cAMP standard by combining 120 μl of diluted sample with 24 μl of 4 M KOH and 6 μl of acetyl anhydride, vortexing for 15 seconds, then adding another 6 μl of KOH and vortexing for 5 seconds, and then placing on ice. Samples were then added to ELISA wells coated with anti-rabbit IgG antibodies, along with either rabbit anti-cGMP or rabbit anti-cAMP antiserum. Tracer molecules of cGMP or cAMP attached to acetylcholinesterase for enzymatic/colorimetric detection were simultaneously incubated to provide competition for binding sites with cell-derived cyclic nucleotides. Wells were then sealed and incubated overnight at room temperature with gentle rocking. After ~18 hours, wells were washed five times each, and color development was performed with Ellman's reagent during an incubation period of ~60 minutes. Absorbance at 410 nm was then measured by SpectraMax M3 spectrophotometer. Values were compared to standard curves to generate an estimated concentration of cGMP or cAMP for each sample. Three biological replicates were performed, each consisting of three technical replicates analyzed for each condition. Data were analyzed by a two-tailed unpooled (Welch's) version of The Student's *t* test to evaluate statistical significance.

Results and Discussion

Profiling of PDE5 Expression, cGMP Signaling, and Vardenafil Dose–Response in Prostate Cancer Cell Lines
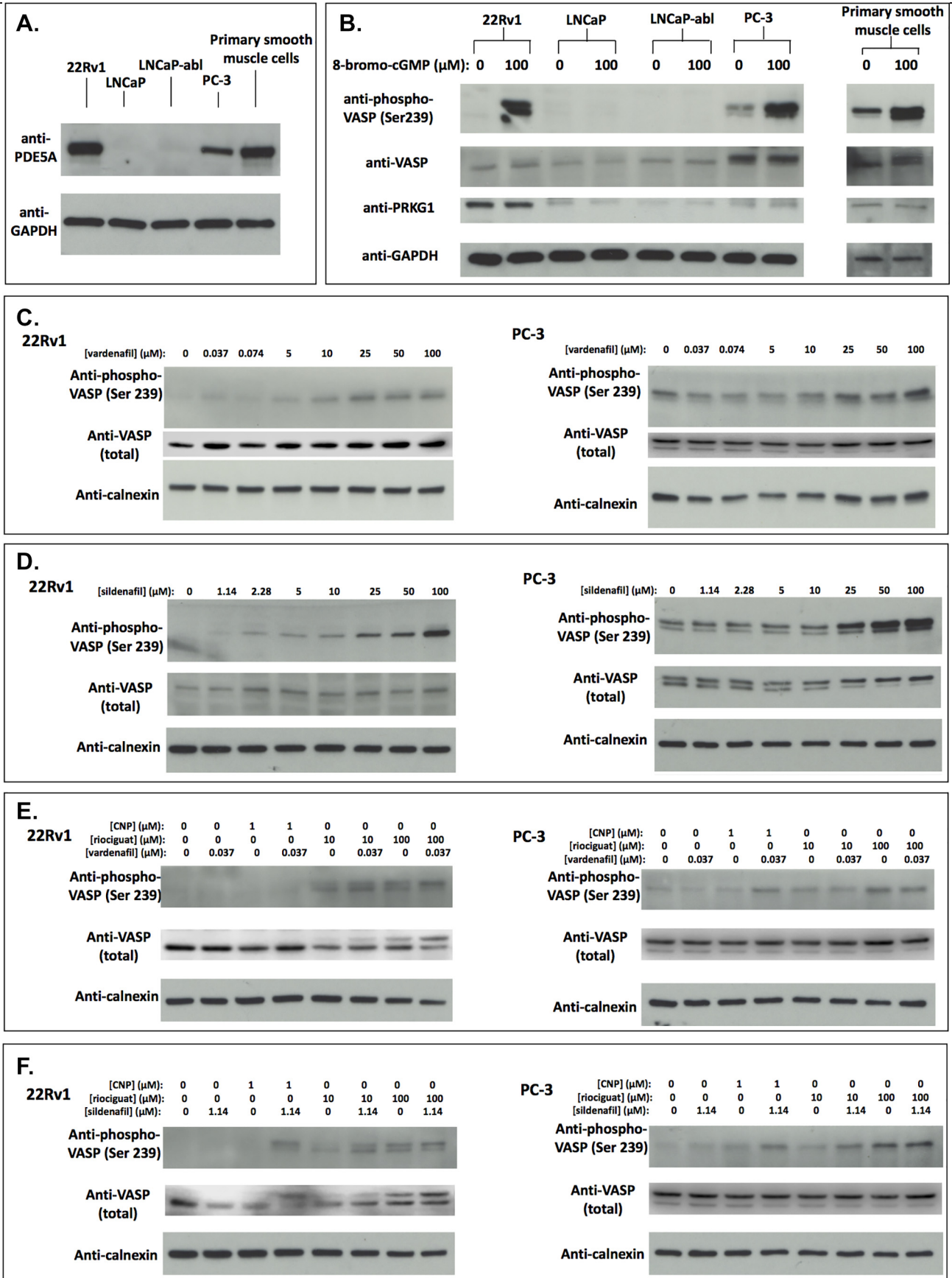
Four cell lines were selected, representing both androgen-dependent (LNCaP) and castration-resistant (LNCaP-abl, 22Rv1, and PC-3) stages of prostate cancer progression. Western blot profiling revealed heterogeneous expression of PDE5 (Figure 1*A*) and a similar expression pattern for cGMP-dependent protein kinase 1 (PRKG1), a key downstream effector of cGMP signaling (Figure 1*B*). Two cell lines highly expressing both PDE5 and PRKG1 (22Rv1 and PC-3) responded robustly to stimulation with a cGMP analog by increasing the phosphorylation of VASP, a well-characterized target of the pathway [16–18], at the Ser 239 residue (Figure 1*B*). In contrast, the two cell lines exhibiting lower expression of the pathway components (LNCaP and LNCaP-abl) did not respond detectably to cGMP stimulation (Figure 1*B*).

Based on these properties, 22Rv1 and PC-3 cells were selected for more detailed molecular characterization following treatment with the PDE5 inhibitors vardenafil and sildenafil. Sildenafil was chosen due to its broad usage (under trade names such as Viagra) and the large body of associated clinical and preclinical literature. Vardenafil was selected for comparison as an increasingly commonly prescribed PDE5 inhibitor (under the trade names Levitra, Staxyn, and Vivanza) that exhibits effectiveness at relatively low doses.

Initially, the minimum concentration of PDE5 inhibitor required to detectably stimulate cGMP accumulation in each cell line was identified (Figure 1, *C* and *D*). This was performed in order to provide insight into the disparity in the literature between PDE5 inhibitor concentrations detected in patient serum and the dramatically higher concentrations used to trigger cGMP accumulation in cell lines. The range of eight different vardenafil concentrations tested was informed by existing clinical studies reporting the maximum concentration of vardenafil found in patient serum as approximately 0.037 μM [19], as well as studies of melanoma cells that triggered cGMP accumulation by administering much higher concentrations between 5 μM [2] and 50 μM [20]. The clinically relevant concentration of 0.037 μM vardenafil was found to be below the minimum concentration threshold necessary to detectably increase VASP phosphorylation at Ser239 during a 1-hour treatment of either 22Rv1 or PC-3 cells (Figure 1*C*).

This experiment was repeated with the alternative PDE5 inhibitor sildenafil (Figure 1*D*). Whereas the clinical literature reports the maximum concentration of sildenafil found in patient serum as approximately 1.14 μM [21], we again found this amount to be below the minimum sildenafil concentration necessary to detectably increase VASP phosphorylation at Ser239 in 22Rv1 or PC-3 cells (Figure 1*C*).

Based on these results, it was unclear whether or not the *in vitro* setting sufficiently models the *in vivo* conditions under which 0.037 μM vardenafil and 1.14 μM sildenafil are therapeutically effective. Primary aortic smooth muscle cells known to be effectively targeted by PDE5 inhibitors in a therapeutic setting were exposed to the same concentration range of vardenafil (Figure S1*A*). Interestingly, these primary cells similarly required a supraclinical concentration of vardenafil to detectably phosphorylate VASP at Ser239 (Figure S1*A*). This requirement was similar to what was observed for 22Rv1 and PC-3 cells and was consistent with the explanation that the *in vitro* environment does not fully recapitulate the *in vivo* one with regard to cGMP signaling. Vascular smooth muscle cells are known to stimulate cGMP synthesis in response to extracellular stimuli such as nitric oxide and natriuretic peptide hormones that can originate from microenvironmental sources such as neuronal and endothelial cells [22,23]. Thus, the clinically relevant concentration of vardenafil may have failed to produce detectable cGMP accumulation in our experiments due to the *in vitro* lack of important extracellular stimuli that are responsible *in vivo* for triggering a sufficient rate of intracellular cGMP synthesis. cGMP synthesis is catalyzed *in vivo* by either soluble or membrane-associated guanylyl cyclase enzymes, which are activated by nitric oxide and natriuretic peptide hormone, respectively. These stimuli can be provided

A.

22Rv1   LNCaP-abl   Primary smooth muscle cells

LNCaP   PC-3

anti-PDE5A

anti-GAPDH

B.

22Rv1   LNCaP   LNCaP-abl   PC-3   Primary smooth muscle cells

8-bromo-cGMP (µM):   0   100   0   100   0   100   0   100   0   100

anti-phospho-VASP (Ser239)

anti-VASP

anti-PRKG1

anti-GAPDH

C.

22Rv1

[vardenafil] (µM)   0   0.037   0.074   5   10   25   50   100

Anti-phospho-VASP (Ser 239)

Anti-VASP (total)

Anti-calnexin

PC-3

[vardenafil] (µM)   0   0.037   0.074   5   10   25   50   100

Anti-phospho-VASP (Ser 239)

Anti-VASP (total)

Anti-calnexin

D.

22Rv1

[sildenafil] (µM)   0   1.14   2.28   5   10   25   50   100

Anti-phospho-VASP (Ser 239)

Anti-VASP (total)

Anti-calnexin

PC-3

[sildenafil] (µM)   0   1.14   2.28   5   10   25   50   100

Anti-phospho-VASP (Ser 239)

Anti-VASP (total)

Anti-calnexin

E.

22Rv1

[CNP] (µM):	0	0	1	1	0	0	0	0
[riociguat] (µM):	0	0	0	0	10	10	100	100
[vardenafil] (µM):	0	0.037	0	0.037	0	0.037	0	0.037

Anti-phospho-VASP (Ser 239)

Anti-VASP (total)

Anti-calnexin

PC-3

[CNP] (µM):	0	0	1	1	0	0	0	0
[riociguat] (µM):	0	0	0	0	10	10	100	100
[vardenafil] (µM):	0	0.037	0	0.037	0	0.037	0	0.037

Anti-phospho-VASP (Ser 239)

Anti-VASP (total)

Anti-calnexin

F.

22Rv1

[CNP] (µM):	0	0	1	1	0	0	0	0
[riociguat] (µM):	0	0	0	0	10	10	100	100
[sildenafil] (µM):	0	1.14	0	1.14	0	1.14	0	1.14

Anti-phospho-VASP (Ser 239)

Anti-VASP (total)

Anti-calnexin

PC-3

[CNP] (µM):	0	0	1	1	0	0	0	0
[riociguat] (µM):	0	0	0	0	10	10	100	100
[sildenafil] (µM):	0	1.14	0	1.14	0	1.14	0	1.14

Anti-phospho-VASP (Ser 239)

Anti-VASP (total)

Anti-calnexin

(caption on next page)

in vitro by media containing either the soluble guanylyl cyclase stimulator riociguat or C-type natriuretic peptide hormone (CNP). Primary aortic smooth muscle control cells responded robustly to stimulation by 10 μM riociguat, 100 μM riociguat, or 1 μM CNP and exhibited enhanced phosphorylation of VASP upon co-treatment with vardenafil at the clinically relevant concentration (Figure S1*B*).

Based on the success of clinically relevant vardenafil concentration when combined with stimulation of cGMP synthesis in the primary cells, 22Rv1 and PC-3 cells were similarly administered vardenafil or sildenafil either alone or in combination with 10 μM riociguat, 100 μM riociguat, or 1 μM CNP (Figure 1, *E* and *F*). Both cell lines exhibited an increased baseline of VASP phosphorylation due to riociguat or CNP, which enabled the clinically relevant concentration of vardenafil (Figure 1*E*) or sildenafil (Figure 1*F*) to trigger an enhancement of VASP phosphorylation. Thus, PDE5 inhibition at clinically relevant concentrations was sufficient to trigger intracellular accumulation of cGMP in prostate cancer cells, at least when co-administered with an agent that stimulates cGMP synthesis.

As a control, the Western blotting experiments depicting dose–response for vardenafil and sildenafil were repeated in low PDE5A-expressing LNCaP and LNCaP-abl cells (Figure S2, *A* and *B*). As predicted, these cell lines activated cGMP signaling less efficiently and less detectably than 22Rv1 or PC-3 cells, requiring long Western blot exposures and high vardenafil and sildenafil concentrations to detect VASP phosphorylation at Ser 239 (Figure S2, *A* and *B*). This indicated that these cell lines are competent to respond at the molecular level to activation of cGMP signaling but do so more modestly. LNCaP and LNCaP-abl cells were then administered PDE5 inhibitor either alone or in combination with 10 μM riociguat, 100 μM riociguat, or 1 μM CNP (Figure S2, *C* and *D*). Both cell lines exhibited an increased baseline of VASP phosphorylation due to high-concentration riociguat. However, it was unclear whether or not the addition of PDE5 inhibitor at a clinically relevant concentration enhanced this VASP phosphorylation (Figure S2, *C* and *D*).

Prostate Cancer Cells Exhibit Stable Phenotypic Responses to PDE5 Inhibition

Based on the results of Figures 1 and S1, we hypothesized that PDE5 inhibitor treatment would not only trigger cGMP accumulation and downstream phosphorylation events but also modify 22Rv1 and PC-3 cellular phenotypes. We were particularly interested in potential cancer-promoting effects corresponding to the reported epidemiologic association between PDE5 inhibitor use and increased prostate cancer recurrence after radical prostatectomy [13]. Initial treatment with vardenafil alone at the clinically relevant concentration did not significantly perturb cellular proliferation (WST-1 assay, Figure 2*A*), colony formation (Figure 2*B*), or migration (wound healing assay, Figure 2*C*). This was true for sildenafil as well (Figure 2, *D-F*).

As a control, the cellular phenotype experiments were repeated in low PDE5A-expressing LNCaP and LNCaP-abl cells (Figure S3). As predicted, these cell lines exhibited minimal responses to PDE5 inhibition (Figure S3), consistent with the conclusion that PDE5 inhibition at clinically relevant concentrations does not dramatically modify cellular proliferation, colony formation, or migration of prostate cancer cells.

Prostate Cancer Cells Exhibit Minimal Phenotypic Responses to PDE5 Inhibition When Co-Treated with a Stimulator of cGMP Synthesis

Based on the lack of molecular response to PDE5 inhibitors at clinically relevant concentrations in the absence of a stimulator of cGMP synthesis (Figure 1, *C-F*), we hypothesized that repeating the studies in Figure 2 with co-administration of riociguat would potentiate the phenotypic effects of PDE5 inhibitor treatment. Surprisingly, co-administration of riociguat did not dramatically enhance the ability of vardenafil (Figure 3, *A-C*) or sildenafil (Figure 3, *D-F*) to modify cellular phenotypes. In instances where a small but statistically significant change was detected (22Rv1 colony formation in Fig. 3, *B* and *E*), the PDE5 inhibitors exerted a tumor-inhibiting rather than tumor-promoting effect, in contrast to epidemiology-based expectations. Overall, PDE5 inhibition at clinically relevant concentrations did not dramatically modify cellular phenotypes such as proliferation, colony formation, or wound healing regardless of whether the drug was administered as a single treatment or in combination with a stimulator of cGMP synthesis.

Genetic Inhibition of PDE5A Triggers Activation of cGMP Signaling and Moderately Counteracts Prostate Cancer Cell Proliferation and Migration

We sought to complement the pharmacological inhibitor data with genetic inhibition of *PDE5A*. Cells were transiently transfected with nontargeting siRNA control pools or with siRNA pools targeting *PDE5A*, *AR*, or *UBE2C* (Figure 4). *AR* was selected as a positive control gene known to drive cancer phenotypes in 22Rv1 cells [24], while the *UBE2C* oncogene served a similar control function for PC-3 cells [25]. Successful knockdown in the *PDE5A* cells was confirmed by Western blotting (Figure S4). Consistent with the findings of higher-dose pharmacological inhibition of PDE5A (Figure 1, *C* and *D*), genetic inhibition increased VASP phosphorylation at Ser239 (Figure S4). Proliferation and migration were assessed using WST-1 (Figure 4*A*) and wound healing assays (Figure 4*B*), respectively. Interestingly, siRNA-based silencing of *PDE5A* significantly inhibited both proliferation and migration, although these effects were relatively weak compared to those of *AR* or *UBE2C* silencing. This finding that *siPDE5A* counteracts prostate cancer cell phenotypes more effectively than PDE5 inhibitor treatment (Figure 2) may indicate that PDE5 activity was blocked more completely by genetic inhibition than by pharmacological inhibition.

Supraclinical PDE5 Inhibitor Treatment Strongly Counteracts Prostate Cancer Cell Phenotypes While Activating Accumulation of cGMP and cAMP

We next measured prostate cancer cell phenotypic responses to supraclinical PDE5 inhibitor concentrations. The body of literature has reported cancer cell phenotypic changes induced by supraclinical

---

← **Figure 1.** Profiling PDE5 expression, cGMP signaling, and PDE5 inhibitor dose–response in prostate cancer cell lines. (A) Four prostate cancer cell lines were examined by Western blotting for PDE5 expression in comparison to a primary aortic smooth muscle cell control known to express the target. α-GAPDH Western blotting served as a loading control. (B) To test the extent to which prostate cancer cells possess an intact cGMP signaling pathway downstream of PDE5, four cell lines were exposed to a cGMP analog and subjected to Western blotting. Primary aortic smooth muscle cells served as a control known to possess a functional cGMP signaling pathway. VASP phosphorylation at Ser239 is a highly specific function of cGMP-dependent kinases that served as a marker of successful cGMP pathway activation. PRKG1 is the cGMP-dependent kinase that exhibits the highest level of expression in prostate cancer and was detected across cell lines as a factor likely to contribute to pathway output. α-Total VASP was performed to confirm approximately equal loading of the total protein between the two treatment conditions for each cell line. α-GAPDH served as a loading control. (C) 22Rv1 and PC-3 cells were subjected to vehicle control treatment, a clinically relevant concentration of vardenafil (0.037 μM), or one of six other supraclinical concentrations over a range previously investigated in the literature. Pathway activation was evaluated by α-phospho-VASP (Ser239) Western blotting with α-total VASP and α-calnexin loading controls. (D) 22Rv1 and PC-3 cells were subjected to vehicle control treatment, a clinically relevant concentration of sildenafil (1.14 μM), or one of six other supraclinical concentrations over a range previously investigated in the literature. Pathway activation was evaluated by α-phospho-VASP (Ser239) Western blotting with α-total VASP and α-calnexin loading controls. (E) 22Rv1 and PC-3 cells were stimulated to increase cGMP synthesis by treatment with either CNP hormone or a high (100 μM) or low (10 μM) riociguat, in the presence or absence of a clinically relevant concentration of vardenafil. (F) 22Rv1 and PC-3 cells were stimulated to increase cGMP synthesis by treatment with either CNP hormone or a high (100 μM) or low (10 μM) riociguat, in the presence or absence of a clinically relevant concentration of sildenafil.
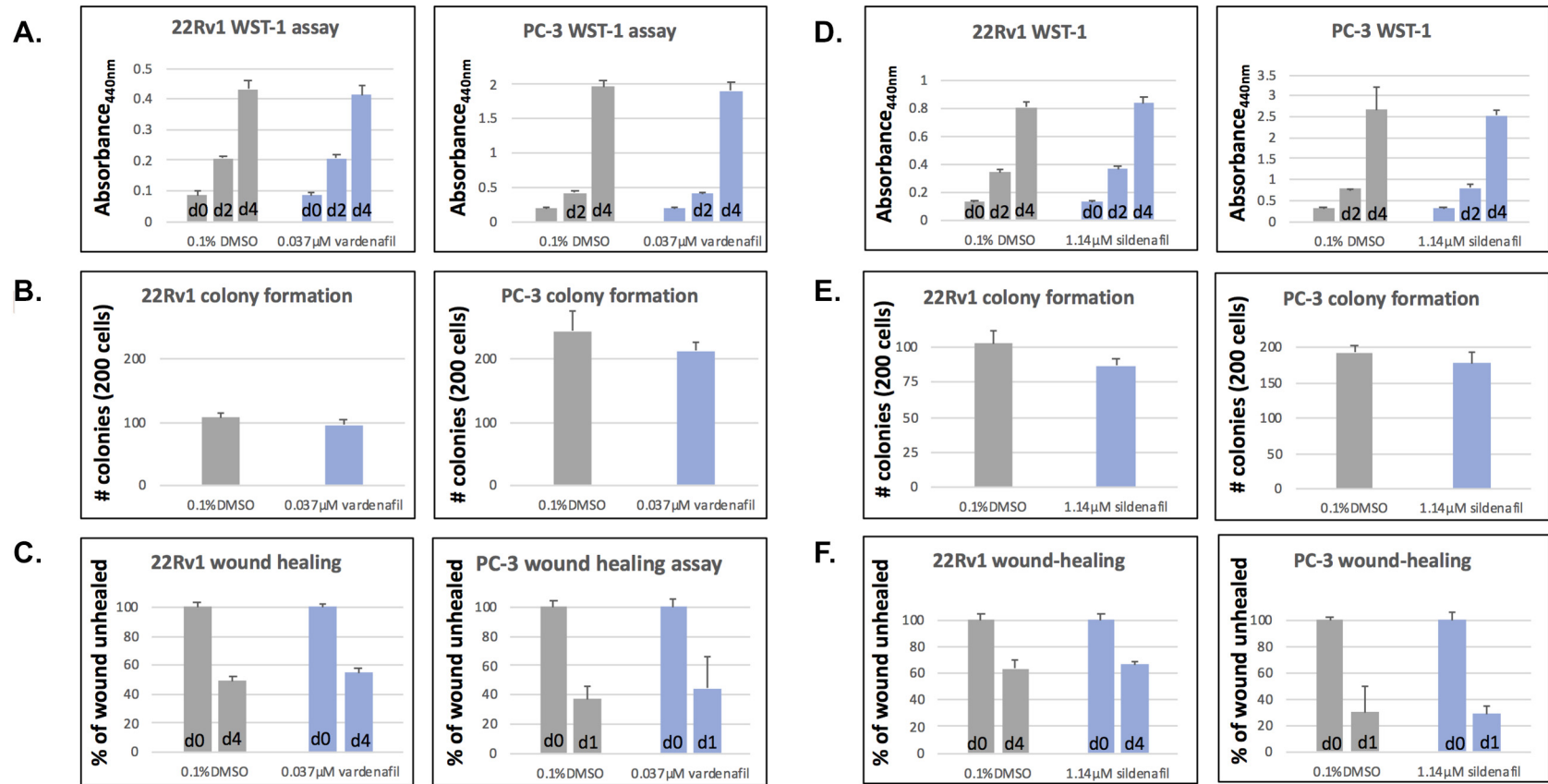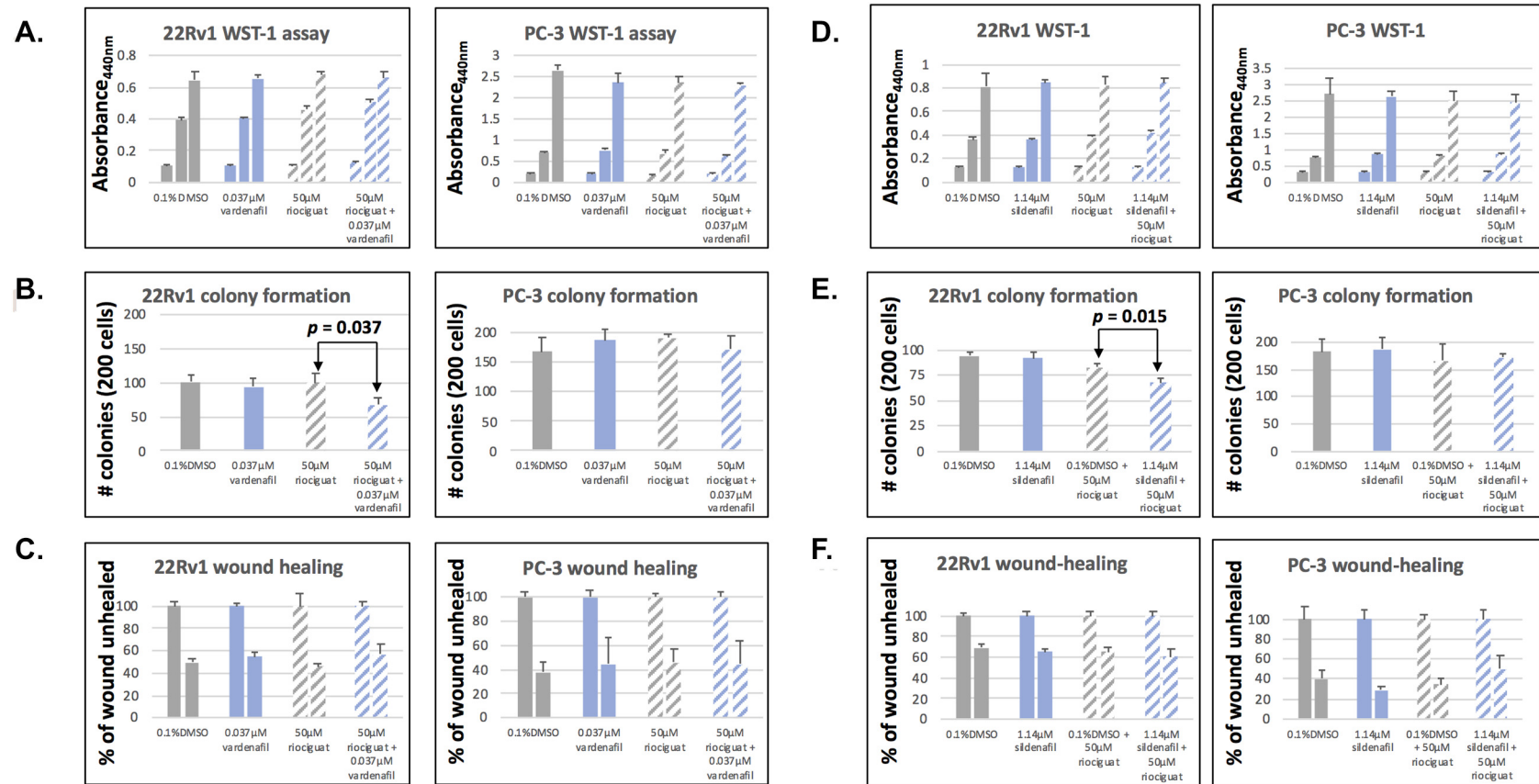
Figure 2. Prostate cancer cell phenotypes remain stable following PDE5 inhibition. Prostate cancer cell phenotypes were examined in three different phenotypic assays in 22Rv1 and PC-3 cells, in the presence or absence of a clinically relevant concentration of vardenafil (0.037 μM) or sildenafil (1.14 μM). Each figure depicts one representative example of two biological replicates, while values are averages of four (WST-1), three (colony formation), or four (wound healing) technical replicates and error bars represent standard deviations. Statistical significance was evaluated using an unpooled two-tailed Student's *t* test and indicated with a *P* value only if ≤ .05. (A/D) WST-1 assay measured the metabolism of a colorimetric substrate by viable cells 0, 2, or 4 days following addition of drug-containing media. (B/E) Colony formation assay measured the efficiency at which 200 seeded cells formed viable colonies at a time point 2 to 3 weeks after addition of drug-containing media. (C/F) Wound healing assay tested cell migration by generating a wound in a confluent monolayer and measuring the percent of its width that remained unhealed at day 0 and at either day 4 (22Rv1) or day 1 (PC-3) after addition of drug-containing media. No comparisons reached statistical significance.

Figure 3. Prostate cancer cells exhibit minimal phenotypic responses to PDE5 inhibition when co-treated with a stimulator of cGMP synthesis. Prostate cancer cell phenotypes were examined in three different phenotypic assays in 22Rv1 and PC-3 cells in the presence or absence of 50 μM riociguat to increase cGMP synthesis and in the presence or absence of a clinically relevant concentration of vardenafil (0.037 μM) or sildenafil (1.14 μM). Each figure depicts one representative example of two biological replicates, while values are averages of four (WST-1), three (colony formation), or four (wound healing) technical replicates and error bars represent standard deviations. Statistical significance was evaluated using an unpooled two-tailed Student's t test and indicated with a P value only if $\leq .05$. (A/D) WST-1 assay measured the metabolism of a colorimetric substrate by viable cells 0, 2, or 4 days following addition of drug-containing media. (B/E) Colony formation assay measured the efficiency at which 200 seeded cells formed viable colonies at a time point 2 to 3 weeks after addition of drug-containing media. (C/F) Wound healing assay tested cell migration by generating a wound in a confluent monolayer and measuring the percent of its width that remained unhealed at day 0 and at either day 4 (22Rv1) or day 1 (PC-3) after addition of drug-containing media. No P value is listed for comparisons that did not reach statistical significance.
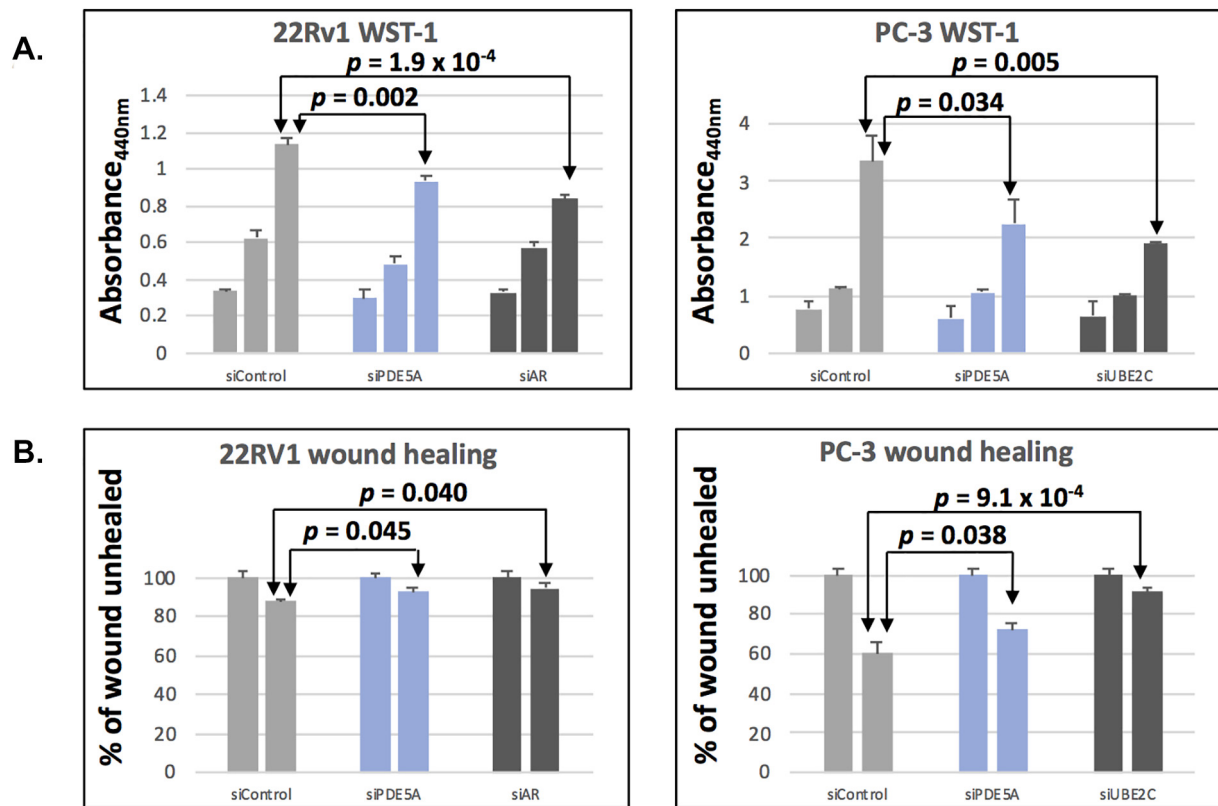
Figure 4. Genetic inhibition of *PDE5A* moderately counteracts prostate cancer cell proliferation and migration. Prostate cancer cell phenotypes were examined in two different phenotypic assays in 22Rv1 or PC-3 cells transfected with nontargeting siRNA control pools or with siRNA pools targeting *PDE5A*, *AR* (only for 22Rv1), or *UBE2C* (only for PC-3). Each value represents the average of four technical replicates, and error bars represent standard deviations. Statistical significance was evaluated using an unpooled two-tailed Student's *t* test and indicated with a *P* value only if $\leq .05$. (A) WST-1 assay measured the metabolism of a colorimetric substrate by viable cells 1, 3, or 5 days following seeding of transfected cells. (B) Wound healing assay tested cell migration by generating a wound in a confluent monolayer of transfected cells and measuring the percent of its width that remained unhealed at day 0 and at either day 4 (22Rv1) or day 1 (PC-3) after wounding.

concentrations of PDE5 inhibitors ranging from 5 µM to 100 µM [2,4–6,20,26,27], including inhibition of PC-3 colony formation by high-dose vardenafil treatment [27]. In the present study, 100 µM vardenafil counteracted proliferation (Figure 5*A*), colony formation (Figure 5*B*), and wound healing (Figure 5*C*) with statistical significance in all cases. High-dose sildenafil triggered similar phenotypic changes in most cases, although with weaker effect sizes (Figure 5, *D-F*). While these concentrations and effect sizes do not model the actual clinical application of vardenafil or sildenafil, it is important to note that their direction is compatible with the weaker effects observed under more clinically relevant conditions (Figures 3 and 4).

Published *in vitro* studies of vardenafil and sildenafil indicate that while they exhibit specificity for PDE5 at the clinically relevant concentration, they each inhibit multiple other phosphodiesterases when present at 100 µM, potentially driving accumulation not only of cGMP but also of cAMP [28]. Cross talk between the cGMP and cAMP signaling pathways also takes place through other known mechanisms [29–31]. The possibility of lost specificity and increased activation of cAMP signaling was investigated by ELISA-based detection of intracellular cGMP and cAMP accumulation following vardenafil treatment (Figure 5, *G* and *H*). As expected, both 22Rv1 and PC-3 cells significantly accumulated intracellular cGMP in response to high-concentration vardenafil treatment (Figure 5*G*), which was correlated with markedly increased phosphorylation of VASP (Figure 1*C*). Both cell lines exhibited moderate but statistically significant cAMP accumulation as well (Figure 5*H*). 22Rv1 showed higher baseline levels of cGMP and stronger cGMP accumulation upon vardenafil treatment relative to PC-3 (Figure 5*G*). Conversely, PC-3 showed higher baseline levels of cAMP and stronger cAMP accumulation relative to 22Rv1 (Figure 5*H*). These results indicated that supraclinical vardenafil treatment predominantly activates cGMP

accumulation, with an accompanying activation of cAMP accumulation that likely represents the sum of off-target effects and indirect cross talk. The inhibitory direction of its effects on prostate cancer cell phenotypes is consistent with the effects of lower-dose PDE5 inhibition, but the molecular mechanisms mediating the higher-dose effects are likely more complex.

Summary of Findings

For approximately 20 years, PDE5 inhibitors have effectively promoted the recovery of reproductive health in prostate cancer patients following prostatectomy or radiotherapy [32,33]. The safety of this practice has been a subject of intermittent research interest, beginning with sildenafil treatment of an orthotopic mouse model of prostate cancer and the finding that tumor growth was not significantly changed in the study [34]. Recent epidemiological reports linking PDE5 inhibitor use to prostate cancer recurrence [13] and melanoma incidence [35] were surprising and alarming but did not culminate in recommendations to change clinical practice for several reasons. The prostate cancer results have proven difficult to reproduce in other cohorts [14,15,36], while the melanoma findings may be confounded by other associated risk-impacting behaviors unaccounted for in the original models [37]. Most importantly, epidemiological evidence for causality such as dose-dependent relationships between the degree of PDE5 inhibitor use and the likelihood of recurrence or the disease stage has been marginal [38] or absent [14,15,39]. The evidence from these retrospective studies has not been sufficient to motivate prospective studies to test for causation, and the relatively few preclinical studies of PDE5 inhibitors in cellular [27] and animal [34] models of prostate cancer have not detected tumor-promoting functions.
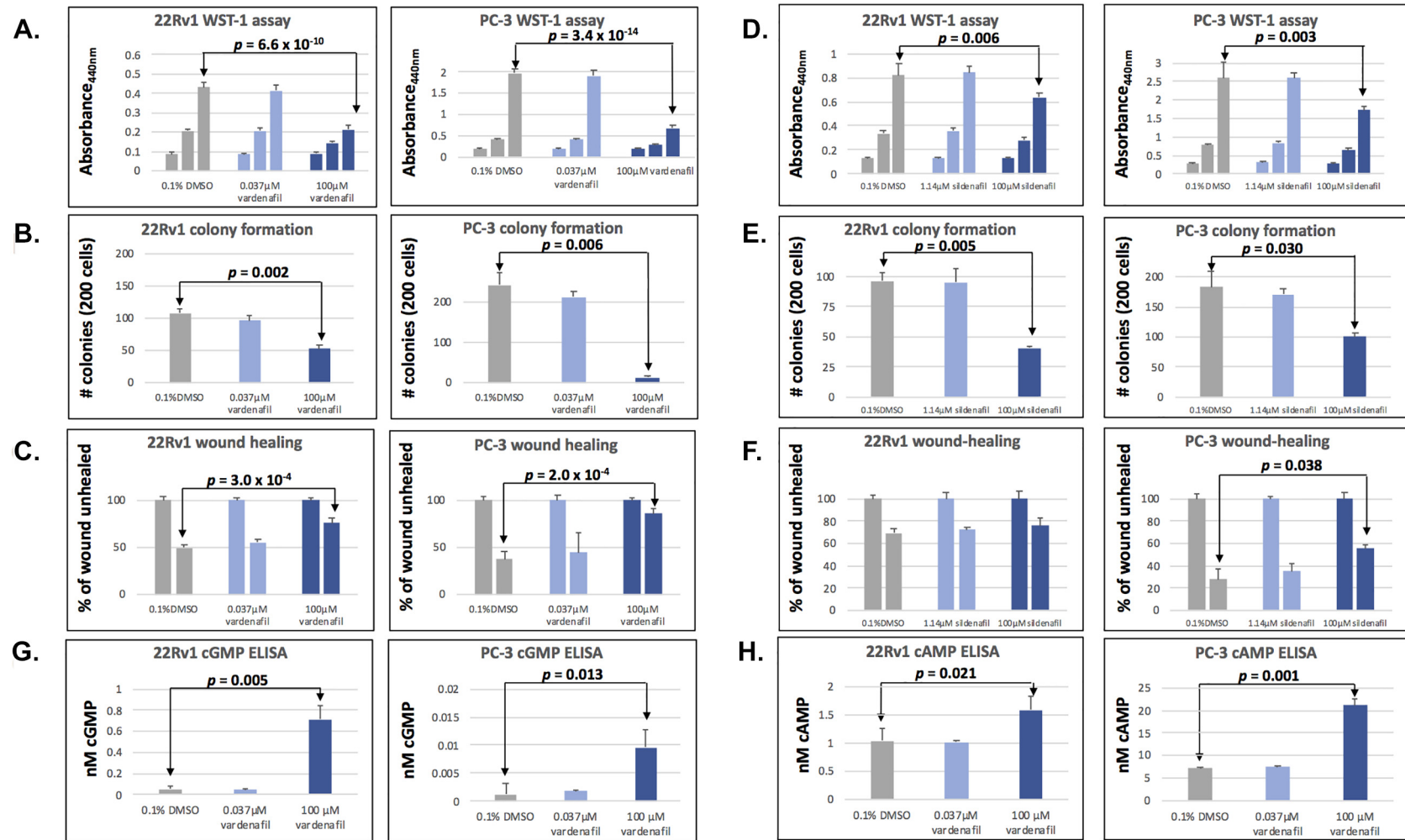
Figure 5. Supraclinical PDE5 inhibitor treatment strongly counteracts prostate cancer cell phenotypes while activating accumulation of cGMP and cAMP. Figures examine prostate cancer cell phenotypes and molecular responses in the presence of PDE5 inhibitor at clinically relevant (0.037 μM vardenafil or 1.14 μM sildenafil) or supraclinical (100 μM of vardenafil or sildenafil) concentrations. Each figure depicts one representative example of two biological replicates. Error bars represent standard deviation. Statistical significance was evaluated using an unpooled two-tailed Student's t test and indicated with a P value only if $\leq .05$. (A/D) WST-1 assay measured the metabolism of a colorimetric substrate by viable cells 0, 2, or 4 days following addition of drug-containing media, and values represent the mean of four technical replicates. (B/E) Colony formation assay measured the efficiency at which 200 seeded cells formed viable colonies at a time point 2 to 3 weeks after addition of drug-containing media. Values represent the mean of three technical replicates. (C/F) Wound healing assay tested cell migration by generating a wound in a confluent monolayer and measuring the percent of its width that remained unhealed at day 0 and at either day 4 (22Rv1) or day 1 (PC-3) after addition of drug-containing media. Values represent the mean of four technical replicates. (G/H) ELISA measured intracellular cGMP or cAMP concentrations in 22Rv1 or PC-3 cells following 60-minute stimulation with vardenafil-containing media. Each experiment depicts the mean of three technical replicates and is representative of three total biological replicates.

This study complements the largely epidemiology-based existing literature on the safety of PDE5 inhibitor use by investigating its potential contributions to prostate cancer recurrence at a cellular and molecular level of detail. Published phenotypic studies of prostate cancer cells [27] and other cell types [2,4–6,20,26] have generally administered PDE5 inhibitors at supraclinical concentrations, while the present study characterizes phenotypic effects at clinically relevant concentrations as well. By monitoring downstream activation of the cGMP signaling pathway at the molecular level, we show that clinically relevant concentrations of PDE5 inhibitors are insufficient *in vitro* to trigger cGMP accumulation on their own (Figure 1, *C* and *D*). Instead, they enhance cGMP accumulation only when combined with the peptide hormone CNP or the soluble guanylyl cyclase stimulator riociguat (Figure 1, *E* and *F*). Both CNP and riociguat increase the baseline of cGMP synthesis so that inhibition of cGMP degradation by PDE5 is more impactful. This co-treatment appears to better approximate endogenous *in vivo* conditions since primary aortic smooth muscle cells, known to be among the key clinical targets of PDE5 inhibition, were similarly unresponsive *in vitro* to a PDE5 inhibitor at clinically relevant concentrations (Figure S1*A*) unless treatment was combined with a stimulator of cGMP synthesis (Figure S1*B*).

Regardless of whether PDE5 inhibitors were administered alone or in combination with riociguat, phenotypic studies repeatedly found no evidence of tumor-promoting effects. Instead, evidence pointed to a weak ability of PDE5 inhibitors to counteract prostate cancer phenotypes, although in most cases these effects failed to reach statistical significance (Figures 2 and 3). siRNA-based *PDE5A* knockdown confirmed with statistical significance both the modest effect size and the tumor suppressive direction of these effects (Figure 4).

On the other hand, PDE5 inhibitor treatment at supraclinical concentrations was strongly inhibitory of all cancer cell phenotypes (Figure 5). Strong activation of cGMP signaling represents one possible mechanism by which this may have occurred. The observed ability of supraclinical PDE5 inhibition to dramatically increase phosphorylation of VASP (Figure 1) at a residue known to inhibit invasion and metastasis in colorectal cancer [40,41] argues that this pathway may contribute at least in part to PDE5 inhibitor antagonism of prostate cancer cellular phenotypes. However, supraclinical PDE5 inhibition also triggered a modest activation of the cAMP pathway, consistent with published reports that higher PDE5 inhibitor concentrations target a wider range of both cGMP- and cAMP-specific PDE enzymes as specificity is lost [28]. Overall, the results emphasize the importance of further studies to characterize the mechanisms by which supraclinical PDE5 inhibitor treatments counteract prostate cancer cell phenotypes, as well as to explore the potential benefits and disadvantages of increased PDE5 inhibitor doses in prostate cancer patients.

The data in this study present an interesting comparison to another recent report showing that VCaP prostate cancer cells exhibit relatively high cGMP synthesis and enhanced cGMP-dependent kinase activity that function to promote their proliferation [42]. The authors showed that this is due to relatively high expression of soluble guanylyl cyclase and that riociguat treatment further promotes proliferation of VCaP (but not LNCaP) cells [42]. While PDE5 inhibitors were not tested in that study, we may extend our future PDE5 studies into other cellular models of prostate cancer.

Conclusions

Collectively, the functional studies presented here argue that the tumor cell autonomous effects of PDE5 inhibition act to suppress rather than promote prostate cancer progression. While this evidence supports the current prevailing concept that PDE5 inhibitor use in the recovery of prostate cancer patients is safe, it is important to acknowledge that these studies do not address or argue against the possibility that PDE5 inhibitors could also contribute to disease progression by acting on other cell types in the more complex *in vivo* tumor microenvironment. For example, a series of interesting studies in brain tumors has found that PDE5 inhibitors can improve capillary permeability within tumors [4]. While this effect has proven useful by enhancing therapeutic delivery and efficacy [43,44], it also may facilitate cell survival and invasion [45]. As a result, we propose that similar future studies be conducted in animal models of prostate cancer, which more fully recapitulate the range of cell types present in the human disease state.

Supplementary data to this article can be found online at https://doi.org/10.1016/j.tranon.2020.100797.

Declaration of Competing Interest

None.

References

[1] M. Drees, R. Zimmermann, G. Eisenbrand, 3′,5′-Cyclic nucleotide phosphodiesterase in tumor cells as potential target for tumor growth inhibition, Cancer Res. 53 (1993) 3058–3061.

[2] I. Arozarena, B. Sanchez-Laorden, L. Packer, C. Hidalgo-Carcedo, R. Hayward, A. Viros, E. Sahai, R. Marais, Oncogenic BRAF induces melanoma cell invasion by downregulating the cGMP-specific phosphodiesterase PDE5A, Cancer Cell 19 (2011) 45–57.

[3] T. Murata, K. Shimizu, Y. Watanabe, H. Morita, M. Sekida, T. Tagawa, Expression and role of phosphodiesterase 5 in human malignant melanoma cell line, Anticancer Res. 30 (2010) 355–358.

[4] M. Sarfati, V. Mateo, S. Baudet, M. Rubio, C. Fernandez, F. Davi, J.L. Binet, J. Delic, H. Merle-Beral, Sildenafil and vardenafil, types 5 and 6 phosphodiesterase inhibitors, induce caspase-dependent apoptosis of B-chronic lymphocytic leukemia cells, Blood 101 (2003) 265–269.

[5] M. Kumazoe, S. Tsukamoto, C. Lesnick, N.E. Kay, K. Yamada, T.D. Shanafelt, H. Tachibana, Vardenafil, a clinically available phosphodiesterase inhibitor, potentiates the killing effect of EGCG on CLL cells, Br. J. Haematol. 168 (2015) 610–613.

[6] M. Kumazoe, Y. Kim, J. Bae, M. Takai, M. Murata, Y. Suemasu, K. Sugihara, S. Yamashita, S. Tsukamoto, Y. Huang, K. Nakahara, K. Yamada, H. Tachibana, Phosphodiesterase 5 inhibitor acts as a potent agent sensitizing acute myeloid leukemia cells to 67-kDa laminin receptor-dependent apoptosis, FEBS Lett. 587 (2013) 3052–3057.

[7] K.A. Noonan, N. Ghosh, L. Rudraraju, M. Bui, I. Borrello, Targeting immune suppression with PDE5 inhibition in end-stage multiple myeloma, Cancer Immunol Res 2 (2014) 725–731.

[8] J.A. Califano, Z. Khan, K.A. Noonan, L. Rudraraju, Z. Zhang, H. Wang, S. Goodman, C.G. Gourin, P.K. Ha, C. Fakhry, J. Saunders, M. Levine, M. Tang, G. Neuner, J.D. Richmon, R. Blanco, N. Agrawal, W.M. Koch, S. Marur, D.T. Weed, P. Serafini, I. Borrello, Tadalafil augments tumor specific immunity in patients with head and neck squamous cell carcinoma, Clin. Cancer Res. 21 (2015) 30–38.

[9] M. Fraser, S.L. Chan, S.S. Chan, R.R. Fiscus, B.K. Tsang, Regulation of p53 and suppression of apoptosis by the soluble guanylyl cyclase/cGMP pathway in human ovarian cancer cells, Oncogene 25 (2006) 2203–2212.

[10] U.C. Garg, A. Hassid, Nitric oxide-generating vasodilators and 8-bromo-cyclic guanosine monophosphate inhibit mitogenesis and proliferation of cultured rat vascular smooth muscle cells, J. Clin. Invest. 83 (1989) 1774–1777.

[11] J.W. Hadden, E.M. Hadden, M.K. Haddox, N.D. Goldberg, Guanosine 3′:5′-cyclic monophosphate: a possible intracellular mediator of mitogenic influences in lymphocytes, Proc. Natl. Acad. Sci. U. S. A. 69 (1972) 3024–3027.

[12] A.H. Chavez, K. Scott Coffield, M. Hasan Rajab, C. Jo, Incidence rate of prostate cancer in men treated for erectile dysfunction with phosphodiesterase type 5 inhibitors: retrospective analysis, Asian J Androl 15 (2013) 246–248.

[13] U. Michl, F. Molfenter, M. Graefen, P. Tennstedt, S. Ahyai, B. Beyer, L. Budaus, A. Haese, H. Heinzer, S.J. Oh, G. Salomon, T. Schlomm, T. Steuber, I. Thederan, H. Huland, D. Tilki, Use of phosphodiesterase type 5 inhibitors may adversely impact biochemical recurrence after radical prostatectomy, J. Urol. 193 (2015) 479–483.

[14] A. Gallina, M. Bianchi, G. Gandaglia, V. Cucchiara, N. Suardi, F. Montorsi, A. Briganti, A detailed analysis of the association between postoperative phosphodiesterase type 5 inhibitor use and the risk of biochemical recurrence after radical prostatectomy, Eur. Urol. 68 (2015) 750–753.

[15] S. Loeb, Y. Folkvaljon, D. Robinson, T. Schlomm, H. Garmo, P. Stattin, Phosphodiesterase type 5 inhibitor use and disease recurrence after prostate cancer treatment, Eur. Urol. 70 (2016) 824–828.

[16] E. Butt, K. Abel, M. Krieger, D. Palm, V. Hoppe, J. Hoppe, U. Walter, cAMP- and cGMP-dependent protein kinase phosphorylation sites of the focal adhesion vasodilator-stimulated phosphoprotein (VASP) in vitro and in intact human platelets, J. Biol. Chem. 269 (1994) 14509–14517.

[17] C. Ibarra-Alvarado, J. Galle, V.O. Melichar, A. Mameghani, H.H. Schmidt, Phosphorylation of blood vessel vasodilator-stimulated phosphoprotein at serine 239 as a functional biochemical marker of endothelial nitric oxide/cyclic GMP signaling, Mol. Pharmacol. 61 (2002) 312–319.

[18] A. Smolenski, C. Bachmann, K. Reinhard, P. Honig-Liedl, T. Jarchau, H. Hoschuetzky, U. Walter, Analysis and regulation of vasodilator-stimulated phosphoprotein serine 239 phosphorylation in vitro and in intact cells using a phosphospecific monoclonal antibody, J. Biol. Chem. 273 (1998) 20029–20035.

[19] T. Klotz, R. Sachse, A. Heidrich, F. Jockenhovel, G. Rohde, G. Wensing, R. Horstmann, R. Engelmann, Vardenafil increases penile rigidity and tumescence in erectile dysfunction patients: a RigiScan and pharmacokinetic study, World J. Urol. 19 (2001) 32–39.

[20] S. Dhayade, S. Kaesler, T. Sinnberg, H. Dobrowinski, S. Peters, U. Naumann, H. Liu, R.E. Hunger, M. Thunemann, T. Biedermann, B. Schittek, H.U. Simon, S. Feil, R. Feil, Sildenafil potentiates a cGMP-dependent pathway to promote melanoma growth, Cell Rep. 14 (2016) 2599–2610.

[21] G.A. Paul, J.S. Gibbs, A.R. Boobis, A. Abbas, M.R. Wilkins, Bosentan decreases the plasma concentration of sildenafil when coprescribed in pulmonary hypertension, Br. J. Clin. Pharmacol. 60 (2005) 107–112.

[22] D.S. Bredt, P.M. Hwang, S.H. Snyder, Localization of nitric oxide synthase indicating a neural role for nitric oxide, Nature 347 (1990) 768–770.

[23] R.M. Palmer, D.S. Ashton, S. Moncada, Vascular endothelial cells synthesize nitric oxide from L-arginine, Nature 333 (1988) 664–666.

[24] Y. He, J. Lu, Z. Ye, S. Hao, L. Wang, M. Kohli, D.J. Tindall, B. Li, R. Zhu, L. Wang, H. Huang, Androgen receptor splice variants bind to constitutively open chromatin and promote abiraterone-resistant growth of prostate cancer, Nucleic Acids Res. 46 (2018) 1895–1911.

[25] Z. Chen, C. Zhang, D. Wu, H. Chen, A. Rorick, X. Zhang, Q. Wang, Phospho-MED1-enhanced UBE2C locus looping drives castration-resistant prostate cancer growth, EMBO J. 30 (2011) 2405–2419.

[26] M. Kumazoe, K. Sugihara, S. Tsukamoto, Y. Huang, Y. Tsurudome, T. Suzuki, Y. Suemasu, N. Ueda, S. Yamashita, Y. Kim, K. Yamada, H. Tachibana, 67-kDa laminin receptor increases cGMP to induce cancer-selective apoptosis, J. Clin. Invest. 123 (2013) 787–799.

[27] N. Liu, L. Mei, X. Fan, C. Tang, X. Ji, X. Hu, W. Shi, Y. Qian, M. Hussain, J. Wu, C. Wang, S. Lin, X. Wu, Phosphodiesterase 5/protein kinase G signal governs stemness of prostate cancer stem cells through Hippo pathway, Cancer Lett. 378 (2016) 38–50.

[28] E. Bischoff, Potency, selectivity, and consequences of nonselectivity of PDE inhibition, Int. J. Impot. Res. 16 (Suppl. 1) (2004) S11–S14.

[29] N.T. Dickinson, E.K. Jang, R.J. Haslam, Activation of cGMP-stimulated phosphodiesterase by nitroprusside limits cAMP accumulation in human platelets: effects on platelet aggregation, Biochem. J. 323 (Pt 2) (1997) 371–377.

[30] G. Kojda, K. Kottenberg, P. Nix, K.D. Schluter, H.M. Piper, E. Noack, Low increase in cGMP induced by organic nitrates and nitrovasodilators improves contractile response of rat ventricular myocytes, Circ. Res. 78 (1996) 91–101.

[31] D.H. Maurice, R.J. Haslam, Molecular basis of the synergistic inhibition of platelet function by nitrovasodilators and activators of adenylate cyclase: inhibition of cyclic AMP breakdown by cyclic GMP, Mol. Pharmacol. 37 (1990) 671–681.

[32] J. Baniel, S. Israilov, E. Segenreich, P.M. Livne, Comparative evaluation of treatments for erectile dysfunction in patients with prostate cancer after radical retropubic prostatectomy, BJU Int. 88 (2001) 58–62.

[33] M.J. Zelefsky, A.B. McKee, H. Lee, S.A. Leibel, Efficacy of oral sildenafil in patients with erectile dysfunction after radiotherapy for carcinoma of the prostate, Urology 53 (1999) 775–778.

[34] C.N. Qian, M. Takahashi, R. Kahnoski, B.T. Teh, Effect of sildenafil citrate on an orthotopic prostate cancer growth and metastasis model, J. Urol. 170 (2003) 994–997.

[35] W.Q. Li, A.A. Qureshi, K.C. Robinson, J. Han, Sildenafil use and increased risk of incident melanoma in US men: a prospective cohort study, JAMA Intern. Med. 174 (2014) 964–970.

[36] J. Jamnagerwalla, L.E. Howard, A.C. Vidal, D.M. Moreira, R. Castro-Santamaria, G.L. Andriole, S.J. Freedland, The Association between Phosphodiesterase Type 5 Inhibitors and Prostate Cancer: Results from the REDUCE Study, J. Urol. 196 (2016) 715–720.

[37] A. Matthews, S.M. Langan, I.J. Douglas, L. Smeeth, K. Bhaskaran, Phosphodiesterase Type 5 Inhibitors and Risk of Malignant Melanoma: Matched Cohort Study Using Primary Care Data from the UK Clinical Practice Research Datalink, PLoS Med. 13 (2016), e1002037. .

[38] Y. Lian, H. Yin, M.N. Pollak, S. Carrier, R.W. Platt, S. Suissa, L. Azoulay, Phosphodiesterase Type 5 Inhibitors and the Risk of Melanoma Skin Cancer, Eur. Urol. 70 (2016) 808–815.

[39] S. Loeb, Y. Folkvaljon, M. Lambe, D. Robinson, H. Garmo, C. Ingvar, P. Stattin, Use of Phosphodiesterase Type 5 Inhibitors for Erectile Dysfunction and Risk of Malignant Melanoma, JAMA 313 (2015) 2449–2455.

[40] Pitari, G. M., Cotzia, P., Ali, M., Birbe, R., Rizzo, W., Bombonati, A., Palazzo, J., Solomides, C., Shuber, A. P., Sinicrope, F. A. & Zuzga, D. S. 2018. Vasodilator-Stimulated Phosphoprotein Biomarkers Are Associated with Invasion and Metastasis in Colorectal Cancer. *Biomark Cancer*, 10, 1179299X18774551.

[41] D.S. Zuzga, J. Pelta-Heller, Li, P., Bombonati, A., Waldman, S. A. & Pitari, G. M., Phosphorylation of vasodilator-stimulated phosphoprotein Ser239 suppresses filopodia and invadopodia in colon cancer, Int. J. Cancer 130 (2012) 2539–2548.

[42] F. Zhou, S. Gao, D. Han, W. Han, S. Chen, S. Patalano, J.A. Macoska, HE, H. H. & CAI, C., TMPRSS2-ERG activates NO-cGMP signaling in prostate cancer cells, Oncogene 38 (2019) 4397–4411.

[43] J. Hu, J.Y. Ljubimova, S. Inoue, B. Konda, R. Patil, H. Ding, A. Espinoza, K.A. Wawrowsky, C. Patil, A.V. Ljubimov, K.L. Black, Phosphodiesterase type 5 inhibitors increase Herceptin transport and treatment efficacy in mouse metastatic brain tumor models, PLoS One 5 (2010), e10108. .

[44] R. Wang, W. Chen, Q. Zhang, Y. Liu, X. Qiao, K. Meng, Y. Mao, Phosphodiesterase type 5 inhibitor Tadalafil increases Rituximab treatment efficacy in a mouse brain lymphoma model, J. Neuro-Oncol. 122 (2015) 35–42.

[45] V. Cesarini, M. Martini, L.R. Vitiani, G.L. Gravina, S. DI Agostino, G. Graziani, Q.G. D'Alessandris, R. Pallini, L.M. Larocca, P. Rossi, E.A. Jannini, S. Dolci, Type 5 phosphodiesterase regulates glioblastoma multiforme aggressiveness and clinical outcome, Oncotarget 8 (2017) 13223–13239.

[46] C.T. Rueden, J. Schindelin, M.C. Hiner, B.E. DeZonia, A.E. Walter, E.T. Arena, K.W. Eliceiri, ImageJ2: ImageJ for the next generation of scientific image data, BMC Bioinformatics 18 (1) (2017) 529, https://doi.org/10.1186/s12859-017-1934-z.